

# Enhancing the interface of cement-paste composite by dispersing sustainable nano-carbon pyrolytic char with silica fume: a sustainable and effective approach

N. K. Karthikeyan<sup>1</sup> and S. Elavenil<sup>2</sup>

<sup>1</sup>Research Associate, School of Civil Engineering, Vellore Institute of Technology, Chennai–campus, Chennai 600127, India

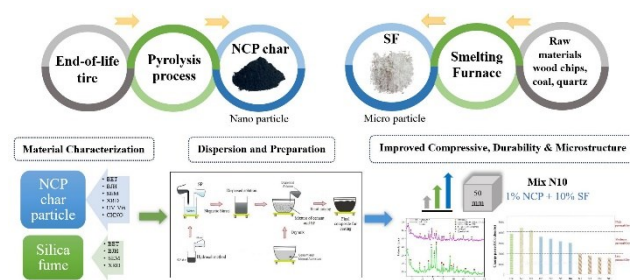
<sup>2</sup>Professor, School of Civil Engineering, Vellore Institute of Technology, Chennai–campus, Chennai 600127, India

Received: 16/12/2023, Accepted: 18/03/2024, Available online: 29/03/2024

\*to whom all correspondence should be addressed: e-mail: elavenil.s@vit.ac.in

<https://doi.org/10.30955/gnj.005662>

## Graphical abstract



## Abstract

Discrete studies are performed on the reuse of end-of-life tires in the construction industry as their accumulation is a global concern to the environment. In consequence, the desired focus of this work is to understand the interaction of powder derived from recycling process of tire waste which yet to be ascertained. The powder yielded through pyrolysis treatment of tire waste is carbon rich and nano in size. On the other hand, Silica Fume (SF) as a micro material is greatly utilized as cement replacement to reduce the environment impact. Therefore, the compressive strength and microstructure properties of cement paste is investigated by incorporating Nano-Carbon Pyrolytic char (NCP) (0.5% & 1%) and SF (0, 2.5, 5, 7.5, 10%) as an additive and filler, respectively, to the weight of cement. The compressive strength of cement paste is ascertained after 1, 3, 7, 14, & 28 days by employing 50mm<sup>3</sup> cube specimen; and the durability properties such as sorptivity, rapid chloride permeability test, and acid test on the samples were examined. Further, Scanning Electron Microscope (SEM) and X-ray Diffraction (XRD) analysis is performed to determine the microstructural properties. Finite element analysis used to model the cubes to validate the experimental findings with analytical results. From the results, the individual addition NCP char (0.5% & 1%) in cement paste reduced the compressive strength of the matrix. Further, the effectiveness of SF directly influences the strength property and separates the agglomerates of

NCP char in cement paste. The cement paste incorporated with 1% of NCP char as Nano and 10% SF as micro blends improved the compressive strength by 18.56%. Furthermore, the Nano/micro blends in cement paste reacts with Ca (OH)<sub>2</sub> to produce dense C-S-H formation due to their reinforcing capability resulting in better durability properties. Finite element analysis exhibit less than 10% of error compared to experimental values. Eventually, the influence of NCP char results in the development of new sustainable nano composites.

**Keywords:** End-of-life tires, pyrolysis treatment, sustainable nanomaterial, nanocomposites, compressive strength, microstructural properties

## 1. Introduction

Portland cement is the foremost construction material produced all over the world, despite the environment carbon footprints that the cement factories leave in this planet (Meyer 2009; Friedlingstein *et al.* 2023). Cement is a binder and a parent material in the concrete production, as it is a predominantly used construction material across the world. However, the quasi-brittle nature of cement based concrete exhibit certain disadvantages such as deficient in resisting crack formation, insufficient tensile strength, durability, ductility and strain capacities. By considering these significant results of cement concrete, recycled materials and by-products of industrial waste are widely applied to enhance cementitious materials (Nalon *et al.* 2022). Moreover, agricultural wastes are also blended as an alternative binder to improve the properties of cement (Kirthiga and Elavenil 2022; Karthikeyan *et al.* 2024; Shanmuga Priya and Padmanaban 2024). In recent years, replacing cement with ultrafine and nano materials has become the mainstream method for sustainable environment (Zhao *et al.* 2015; Jegatheeswaran *et al.* 2023; Kanagasundaram and Solaiyan 2023).

In this regard, discrete investigation by researchers has been carried out to provide various solution to recycle and utilize all types of waste materials in to cement matrix (Nalon *et al.* 2022; Naveen Arasu *et al.* 2023). Among the

abundant waste materials, one of the interesting wastes is end-of-life tires which is a non-biodegradable material produced in millions per year worldwide (Valentini and Pegoretti 2022). Considerably, India, China, USA, and Europe recover the most end-of-life tyres (WBCSD 2019). Although the end-of-life tires are recycled, most of the tires are accumulated into landfills causing contamination to the soil, air, and water. Subsequently, numerous studies were carried out by using tire waste as a partial replacement for fine and coarse aggregate in the form of crumb and shredded rubber, respectively (Hamdi *et al.* 2021; Ren *et al.* 2022). However, the ultrafine rubber particles as a partial replacement for cement which is obtained through burning of tyres at 500°C (pyrolysis) has not yet ascertained. The effectiveness of NCP char as a carbon source depended on the interaction of pyrolysis conditions (Kouimtzi and Kostopoulou 2023) as it could determine the physical and chemical properties. Successful incorporation of pyrolytic carbon in cement can absorb stress, prevents shrinkage deformation, and can resist micro-cracks (Chen *et al.* 2014; Huang *et al.* 2014). Therefore, NCP char could be promising application in cementitious matrix prospect.

A few research work focussed on using end-of-life tires in powder form as a partial replacement for cement. Influencing the tire powder as a cement replacement is an ideal way that could be used in various applications such as sub-base, base, retaining walls, and rammed earth. Comparatively, using 5% of ground tire rubber in cement leads to a significant reduction in compressive strength of concrete due to less dosage of cement (Gil-Martín *et al.* 2019; Zafar *et al.* 2022). However, tire powder emits low CO<sub>2</sub> and less in material cost. Whereas, the cement clay composites with optimum of 2.5% tire powder empowers ductile behavior, compressive strength, shear modulus, and elastic modulus. But decrease in the compressive strength was also greatly noted, which has become major concern in utilizing tire rubber powder (Al-Subari *et al.* 2021). Moreover, degradation in load carrying capacity of beam-column joint using ground tire rubber was also noticed under cyclic behaviour (Gil-Martín *et al.* 2019). Most of the studies have concluded that the tire rubber in cement has decreased the mechanical strength of cementitious composites. Since it is hydrophobic and has strong surface inertia, the interface between the tire rubber powder and cement matrix is abnormal. To minimize such adverse effect, a study explored by modifying or treating the tire rubber powder using physical cleaning and chemical cleaning methods to improve hydrophilicity and polarity, respectively. This successful modification methods enhanced the surface activation and hydrophilicity that increases the compressive, flexural, and toughness of cement mortar (Zhang *et al.* 2022a). Inherently, tire rubber powder inhibit the cement reaction in the hydration process. Because, the presence of Zn in rubber tire particle will slow down the acceleration of C<sub>3</sub>S process.

Simultaneously, researchers found that using tire rubber powder with another waste materials, which is a global concern to environment impact is advantageous as it can

improve the properties of waste rubber powder without additional treatments. It was observed that binary blends (fluorogypsum + tyre rubber powder) in cement mixture regulates the hydration process which recover 28% and 36% in compressive strength and modulus of elasticity, respectively (R *et al.* 2021). Subsequently, in another study, when waste tire rubber powder of 2.5% is directly mixed to cement fraction, the compressive strength of the mortar is reduced. While, the addition of polypropylene fibre with waste tire powder exhibit excellent synergistic effect to improve compressive strength of mortar and alleviates the damage caused by alkali-silica reaction than the inhibitory effect of lone blends (Gao *et al.* 2023). From extensive experimental studies, it is clear that NCP char as cement replacement reduces the dosage of cement content and resist hydration process. Therefore, NCP char should be included as an additive instead of replacement to cement and a suitable filler as a secondary binder is required to assist hydration process in the cement matrix. In this regard, there are by-products produced from various industries that are used as a secondary binder for cement to enhance the microstructure and engineering properties. The several recycled waste materials such as fly ash (Liu *et al.* 2023), red mud (He *et al.* 2024), metakaolin (Luo and Wei 2023), biochar (Wang and Wang 2023), silica fume (Ma *et al.* 2022), sludge (Xia *et al.* 2023), calcined clay (Murali *et al.* 2023), and slag (Zhang *et al.* 2023) are used as a secondary binder to cement. Moreover, these materials are used in binary and ternary system of binder materials to improve the hydration characteristics to enhance the mechanical properties (Zhu *et al.* 2014). Among the other binder materials, the presence of SF in cement matrix results in high pozzolanic reaction over the portlandites, further developing more secondary C-S-H formation (Vashistha *et al.* 2023). The addition of SF as a replacement to cement can significantly improve the engineering properties of cement paste matrix compared to other binders (Luo *et al.* 2022). The effective dosage of SF in cement paste can perform better at micro and nanostructure despite with low water to binder ratio (Zhang *et al.* 2022b). Moreover, the SF has the ability to disperse agglomerates of nano carbon materials with escalated thermal expansion and high silica content (Kim *et al.* 2019; Dong *et al.* 2020). But the obvious concentration of silica content to disperse nano agglomerates has to be ascertained for NCP char. Therefore, varying the amount of silica content with respect to change in NCP char is to be investigated.

Numerous studies have been carried out by employing and modifying the tire rubber powder in different concentrations. However, the limitations and research gaps are significantly noticed in the existing research using NCP char. Initially, the research on Nano sized carbon based pyrolytic char as an additive to cement on strength properties is not identified. Further, no research work have emphasized the characterization of NCP char in examining the nano properties and its effective dispersion in the cement composites. Moreover, as of yet, the durability properties of cement composites using NCP char is also not addressed to study to resilience of the nano particle. On the

other hand, environmental constraints are performed for structural components (Lokesh *et al.* 2023) but validating the nano composites using finite element modelling is not distinguished. With the focus of evaluating such sustainable nanomaterial in cementitious matrix, this paper investigates the mechanical and durability characteristic of cement paste influencing NCP char, and SF as binary blends for dispersion purpose. The effect of SF in improving the compressive strength and dispersing NCP char in the cement matrix without agglomerates is determined and the experimental findings are validated using finite element modelling analysis. In addition, microstructure characterization using SEM and XRD is performed to know the interface between cement and binary blends. Eventually, by utilizing NCP char as nanomaterial and SF as micro materials, the synergistic effect will lead to development of sustainable nano cement composites.

**2. Research significance**

The role of NCP char as sustainable nano carbon particle in cement composite is not as of yet reported. Furthermore, none of the research work has emphasized the utilization of NCP char to enhance the mechanical and durability properties. Therefore, the current novelty of the study is to introduce NCP char as sustainable nanomaterial into cement matrix. The objective of this research includes four aspects. Firstly, examining the properties of sustainable NCP char using various characterization techniques to perform as sustainable nanomaterial. Secondly, verifying the effect of compressive strength of cement paste composites on adding NCP char, dispersion process, and NCP char/SF, respectively. Thirdly, analyzing the important

durability properties and microstructure of cement composites for the selected mixes. To achieve these goals, cement paste composites with different volume percentage of NCP char ranging from 0% to 1% of weight and SF ranging from 0% to 10% of weight were fabricated by simple mechanical method. Fourthly, constructing a finite element model to validate the experimental findings is executed. Ultimately, the synergistic effect of NCP char and SF were experimentally studied to develop sustainable nano composites.

**3. Materials and mix proportions**

*3.1. Materials*

Experiments were conducted on cement paste matrix, which is a mixture of Ordinary Portland Cement (OPC), SF, and NCP char with varying substitution levels, and the available tap water in the laboratory at room temperature was used for mixing cementitious paste. Polycarboxylate Ether (Master EASE) was added to the mixture to disperse the NCP char without agglomerates and to regulate the workability of cement paste.

*3.1.1. Cement*

The cement utilized was OPC having the strength grade of 53, produced by Chettinad Cement Co. Ltd, India, conforming to the requirements of IS 12269-2013. The physical property tests on cement were determined by different IS 4031 test method and it satisfies all the requirements as shown in Table 1. Moreover, chemical property test on cement is determined by oxide composition using X-Ray Fluorescence (XRF) spectroscopy which is presented in the Table 2.

**Table 1.** Physical properties of OPC as per IS 12269–2013

| Physical properties    |                       | Requirements as per IS 12269–2013 | Test methods |
|------------------------|-----------------------|-----------------------------------|--------------|
| Specific gravity       | 3.14                  | 3.10-3.15                         | IS 4031– 11  |
| Fineness               | 4%                    | <10%                              | IS 4031 - 1  |
| Soundness              | 7mm                   | Max 10mm                          | IS 4031 – 3  |
| Consistency            | 31%                   | 30-35%                            | IS 4031 – 4  |
| Setting time (Initial) | 75min                 | Min. 30minutes                    | IS 4031 - 5  |
| Setting time (Final)   | 365min                | Max. 600minutes                   | IS 4031 – 5  |
| Compressive strength   | 54.4N/mm <sup>2</sup> | 53 N/mm <sup>2</sup> @28days      | IS 4031 - 6  |

**Table 2.** Chemical composition of OPC

| CaO   | SiO <sub>2</sub> | Fe <sub>2</sub> O <sub>3</sub> | Al <sub>2</sub> O <sub>3</sub> | SO <sub>3</sub> | MgO  | K <sub>2</sub> O | Na <sub>2</sub> O | LOI  |
|-------|------------------|--------------------------------|--------------------------------|-----------------|------|------------------|-------------------|------|
| 66.54 | 19.04            | 5.04                           | 4.46                           | 2.45            | 0.91 | 0.39             | 0.12              | 1.05 |

**Table 3.** Physical properties and XRF composition of NCP char

| Physical properties |      |                                |                   |                                |      |                  |                  |                               |         |      |
|---------------------|------|--------------------------------|-------------------|--------------------------------|------|------------------|------------------|-------------------------------|---------|------|
| Appearance          |      |                                |                   |                                |      | Black            |                  |                               |         |      |
| Specific gravity    |      |                                |                   |                                |      | 1.89             |                  |                               |         |      |
| Fixed Carbon        |      |                                |                   |                                |      | > 80%            |                  |                               |         |      |
| DBP oil absorption  |      |                                |                   |                                |      | 110ml/100g       |                  |                               |         |      |
| pH value            |      |                                |                   |                                |      | 6.3              |                  |                               |         |      |
| Porosity            |      |                                |                   |                                |      | 2.6%             |                  |                               |         |      |
| Oxide composition   |      |                                |                   |                                |      |                  |                  |                               |         |      |
| SiO <sub>2</sub>    | CaO  | Fe <sub>2</sub> O <sub>3</sub> | Na <sub>2</sub> O | Al <sub>2</sub> O <sub>3</sub> | MgO  | TiO <sub>2</sub> | K <sub>2</sub> O | P <sub>2</sub> O <sub>5</sub> | MnO     | LOI  |
| 7.01                | 0.99 | 0.91                           | 0.58              | 0.55                           | 0.16 | 0.14             | 0.11             | 0.073                         | 55.9PPM | 81.5 |

**Table 4.** Chemical composition of SF

| SiO <sub>2</sub> | Al <sub>2</sub> O <sub>3</sub> | CaO  | K <sub>2</sub> O | Fe <sub>2</sub> O <sub>3</sub> | MgO    | Na <sub>2</sub> O | P <sub>2</sub> O <sub>5</sub> | TiO <sub>2</sub> | MnO | LOI  |
|------------------|--------------------------------|------|------------------|--------------------------------|--------|-------------------|-------------------------------|------------------|-----|------|
| 98.6             | 0.49                           | 0.17 | 0.15             | 0.0373                         | 0.0321 | 0.028             | 0.0139                        | 62.6PPM          | ND  | 0.47 |

### 3.1.2. NCP char

The raw NCP char particle acquired from pyrolysis plant was sponsored by GS Pyro Enterprise Pvt. Ltd., India. NCP char was used as a carbon based nano functional filler for fabrication of nano cementitious composites. The physical properties and XRF composition of NCP char is shown in Table 3. The Figure 1 shows the photograph and micrograph of NCP char.

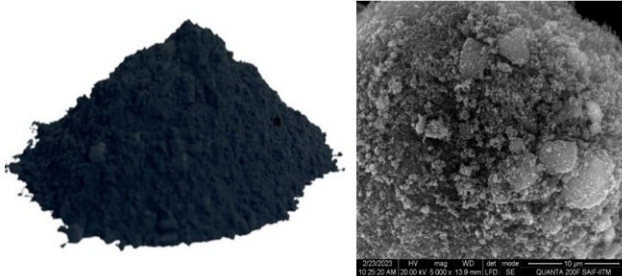


**Figure 1.** Photograph and Scanning electron microscope image of NCP char

### 3.1.3. Silica fume

The SF (white) is used as a binder and filler to improve the microstructure properties and to attain high pozzolanic reaction, respectively. Moreover, SF with high silica content has the capability to separate the agglomerates of nano particles. The SF having average particle size of  $1\mu\text{m}$  and specific gravity of 2.2 was obtained from Astraa Chemicals, Chennai, India. Figure 2 represents the image and micrograph of silica fume. The chemical composition of silica fume by XRF spectroscopy is shown in Table 4.



**Figure 2.** Photograph and SEM image of SF

### 3.2. Mixing proportions

In this experimental work, cement paste matrix was investigated by incorporating nano carbon powder (NCP char). In this regard different mixes were produced to determine the compressive strength of the matrix. Further, the water-binder (w/b) ratio employed for all the mixtures was 0.29. While preparing the cementitious mixture, the NCP char particle was added in percentage of 0.5% and 1% of the total cement volume. Meanwhile, OPC was replaced with SF in percentage of 0%, 2.5%, 5%, 7.5%, & 10% of the total cement volume to evaluate the dispersion of NCP char in the cement paste. The Table 5 summarizes the mixing proportions that are adopted to design the cementitious composites. Whereas, CC refers the controlled cement paste matrix and the different mix proportions are represented as Mix ID, N1 – N10.

**Table 5.** Various mix proportion adopted for cementitious composites

| Mix ID | Cement (g) | SF (g) | NCP char (g) | Water (ml) | SP (ml) |
|--------|------------|--------|--------------|------------|---------|
| CC     | 216        | -      | -            | 62.64      | -       |
| N1     | 216        | -      | 1.08         | 62.64      | 1.08    |
| N2     | 216        | -      | 2.16         | 62.64      | 2.16    |
| N3     | 210.6      | 5.4    | 1.08         | 62.64      | 1.08    |
| N4     | 210.6      | 5.4    | 2.16         | 62.64      | 2.16    |
| N5     | 205.2      | 10.8   | 1.08         | 62.64      | 1.08    |
| N6     | 205.2      | 10.8   | 2.16         | 62.64      | 2.16    |
| N7     | 199.8      | 16.2   | 1.08         | 62.64      | 1.08    |
| N8     | 199.8      | 16.2   | 2.16         | 62.64      | 2.16    |
| N9     | 194.4      | 21.6   | 1.08         | 62.64      | 1.08    |
| N10    | 194.4      | 21.6   | 2.16         | 62.64      | 2.16    |

## 4. Experimental method

### 4.1. Characterization of NCP char and SF

The NCP char is carbon-based char derived after the waste tire pyrolysis treatment. On the other hand, the SF is obtained after the smelting furnace and baghouse filter of various raw material includes coal, wood chips, quartz, etc. Since, NCP char and SF has high carbon and silica content, respectively. The mechanism of these materials substantially involves and varies in several parameters such as surface area, pore size distribution, surface morphology, crystallinity and different chemical phases. Therefore, NCP char and SF is evaluated using different characterization techniques such as Brunauer-Emmett-Teller (BET) model,

Barrett Joyner Halenda (BJH) model, X-ray Powder Diffraction (XRD), and Scanning Electron Microscope (SEM). Additionally, Ultra Violet – Visible (UV-Vis) spectroscopy and CHNSO analysis were performed on NCP char to determine quality and carbon content.

### 4.2. Dispersion method and preparation of sample

Hand mixing was employed to prepare cement paste with NCP char and SF. The preparation procedure for casting the cement paste specimen using first admixing method (Kanagasundaram and Solaiyan 2023) is performed according to requirements and standard as shown in Figure 3. The step-by-step procedure as follows: I) mix super plasticizer with the water and stir well until completely mixed. II) add NCP char solution in to mixed solution and

disperse using magnetic stirrer for 4 hours period, while mixing at slow speed (250rpm) for 2 hours and high speed (350rpm) for 2 hours. III) On the other hand, dry mix the cement with SF until it is homogeneously mixed. IV) Now add dispersed solution and mix the paste until it is homogenized. V) Pour the fresh cement paste into the cube moulds. Further, the specimen was cast and hand compacted in three gang moulds having 50 mm X 50 mm X 50 mm of size. The specimen was demoulded after 24 hours and continued the water curing process until 28 days under room temperature.

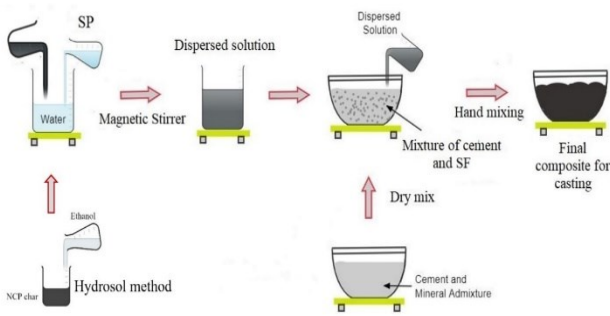


**Figure 3.** Preparation of cementitious composites using first admixing dispersion method



**Figure 4.** Test setup of CTM for compressive strength

**4.3. Compressive strength**

In order to inspect the influence of incorporating NCP char and combination of NCP char with SF on the strength properties of cement paste cubes, the compressive strength was performed on cube specimen (50 X 50 X 50 mm) at the ages of 1 day, 3 days, 7 days, 14 days, and 28 days according to the ASTM C109. The test setup of Concrete Testing Machine (CTM) is depicted in the Figure 4. In order to know the importance of dispersion technique, the variations in the compressive strength with and without dispersion process were also compared and discussed. The CTM with a capacity of 2000 kN was used for compressive testing, while the loading rate was maintained at 0.2 N/mm<sup>2</sup>/sec and five samples were repeated for all the ages of test. The initial test speed and constant start is set to 0.1mm/sec and 20 kN, respectively.

**4.4. Durability properties**

The durability properties of cement paste matrix with NCP char and NCP/SF is determined based on sorptivity, Rapid Chloride Permeability Test (RCPT), and acid attack test. The

sorptivity test was carried out on sample 100mm x 50mm disc after 28 days of curing. The side and upper surface of the disc was protected with epoxy and plastic tape, respectively, prior to dipping the exposed surface of the disc into water up to 3-5mm from bottom as shown in Figure 5a. Then the sorptivity (rate of absorption) was measured at different intervals of time according to ASTM C1585 – 04. Similarly, RCPT was experimented on 100mm x 50mm disc in accordance with ASTM C1202-19 to study the resistance of cement composite to the penetration of chloride ions. This experiment was lasted for 6 hours at room temperature to acquire adequate results as shown in Figure 5b. Meanwhile, 50mm<sup>3</sup> cubes were casted and cured for 28 days to conduct acid attack test. Further, the cubes were removed from curing and immersed completely in the diluted nitric acid (1.5%) as depicted in Figure 5c. The cubes were inspected visually and the mass loss was measured after 1, 3, 7, 14, and 28 days.

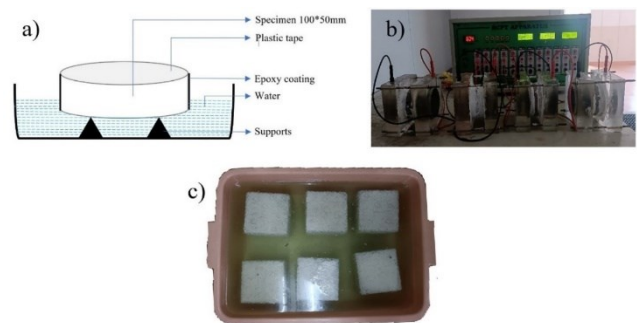


**Figure 5.** Experimental setup a) Sorptivity b) RCPT c) Acid test

**4.5. Microstructural properties**

SEM analysis was performed to reveal the mechanism of hydrated morphology and presence of defects at micro-scale. Moreover, microstructure properties of cement paste were analysed using SEM to identify the complete distribution of NCP char in the cement matrix. It also provides essential insights on pores and hydration products to ensure the performance of NCP/SF in the cement matrix at nanoscale. SEM was carried out using QUANTA 200F instrument with an accelerated voltage of 30 kV and Secondary Electron (SE) imaging was performed. The microstructure properties were determined for the sample mix with high compressive strength. Furthermore, the correlation between the SF and hydration products can be ascertained. Meanwhile, XRD analysis were performed using a RIGAKU Smartlab 3kW (200V, 50/60 Hz, 3Φ 30A) instrument to validate the presence of hydration products and various phases in the cement matrix by phase identification with Xpert Hi-score software.

**5. Finite element analysis**

Finite Element Analysis (FEA) is a computational technique used primarily to simulate and analyse the behaviour of concrete structures or elements under various loading conditions. In addition, FEA is also used to study the analytical behaviour of material when incorporated into cement matrix under loading conditions, say compressive or flexural. In this work, ANSYS 2021 R2 (Workbench) version is utilized for FEA for discretizing complex geometrics into finite elements by applying boundary

conditions. Further, ANSYS facilitate to accurately predict the stress, strain, and distribution of deformations within the cement matrix. Its comprehensive post-processing tools and algorithms helps to visualize the simulation results and carry out in-depth analysis on the properties of cement matrix. Therefore, FEA is performed on the conventional cement paste matrix (CC) and NCP char-based cement paste matrix (N10) having highest strength for validating the experimental values with analytical results under compressive loading.

## 6. Results and discussion

### 6.1. Characterization of NCP char and SF

The possible characterization techniques were adopted to investigate the various parameters of NCP char and SF. The BET plots as shown in Figure 6a and 6b indicates  $29.5 \text{ m}^2/\text{g}$  &  $3.86 \text{ m}^2/\text{g}$  of surface area,  $0.051 \text{ cm}^3/\text{g}$  &  $0.005 \text{ cm}^3/\text{g}$  of total pore volume, and  $7.678 \text{ nm}$  &  $4.986 \text{ nm}$  of mean pore diameter for both NCP char and SF, respectively. Meanwhile, the BJH plots as depicted in Figure 7a and 7b exhibits the pore size distribution values of  $1.22 \text{ nm}$  &  $2.12 \text{ nm}$  for NCP char and SF, respectively. Moreover, the SEM image in Figure 8a shows that the NCP char having visuals of spherical shape and regular surface morphology with interconnected grape like structure. The average particle size of UPC and SF are  $\sim 56 \text{ nm}$  and  $< 1 \mu\text{m}$ , respectively, which are determined from the Figure 8a and 8 b using ImageJ software. Furthermore, the XRD pattern of NCP char is shown in Figure 9. The peaks ( $2\theta^\circ$ ) were identified and matched with different crystalline mineral phases and found that the major of the peaks are associated to ZnS (Zinc sulphide) (JCPDS card no. 01-077-2100) due to sulfidation (Shilpa *et al.* 2018; Wang *et al.* 2019). Further, the pure carbon (JCPDS card no. 01-072-2091) and graphite (JCPDS card no. 01-075-2078) phases were also determined and matched next to ZnS. Noticeably, the broader peaks between  $40^\circ$  to  $50^\circ$  and  $20^\circ$  to  $30^\circ$  represents the presence of high amount of amorphous carbon (Nogueira *et al.* 2019).

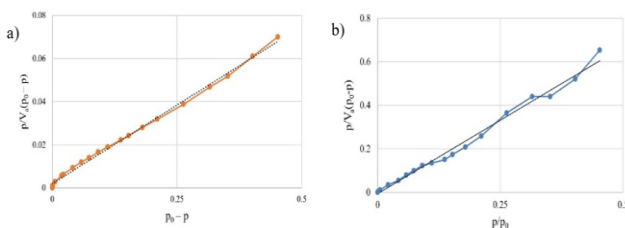


Figure 6. BET plot a) NCP char b) SF

On the other hand, the Figure 10 shows the XRD pattern of SF, where all the peaks ( $2\theta^\circ$ ) are attributed  $\text{SiO}_2$  which states the presence of high amount of amorphous silica in the material (Khater 2013). The UV-Vis absorbance spectra vs wavelength is performed on NCP char as depicted in Figure 11. The display of continuous and good absorption of light rays throughout the wavelength region from  $200 \text{ nm}$  to  $800 \text{ nm}$  exhibits the presence of pure carbon in NCP char. Furthermore, the CHNO analysis revealed the presence of high carbon content which is  $>80\%$  in the NCP char. The results of characterization shows the potential ability of NCP char with its nano size having high carbon

content and SF with high amorphous silica can influence strength and microstructure of the cement matrix.

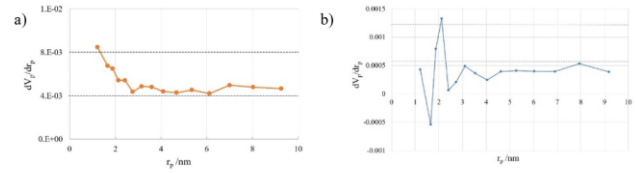


Figure 7. BJH plot a) NCP char b) SF

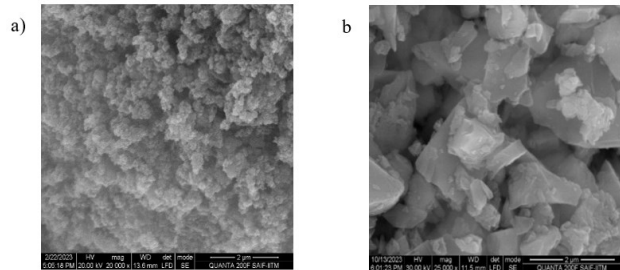


Figure 8. SEM micrographs a) NCP char b) SF

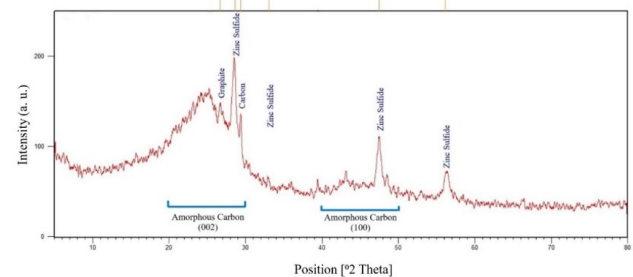


Figure 9. XRD phase identification of NCP char

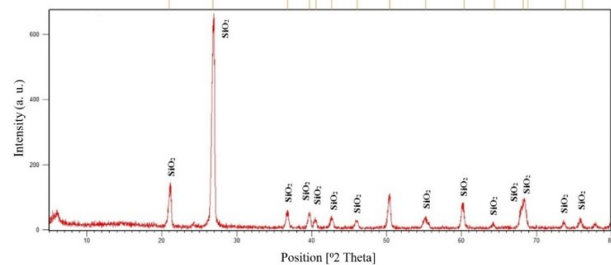


Figure 10. XRD phase identification of SF

### 6.2. Compressive strength

#### 6.2.1. Effects of compressive strength on adding NCP char

The strength of the cement paste cubes integrated with NCP char were tested for the age 1, 3, 7, 14, & 28 days is depicted in the Figure 12. In addition, linear expressions are established and correlated in Figure 12 to understand the relationship of compressive strength with the age of curing. The addition of 0.5% and 1% of NCP char in cement has significantly reduced the compressive strength of the cement matrix at 1, 3, 7, 14, & 28 days when compared to conventional mix, which was decreased by 28%, 30%, 36%, 31%, 36% for N1 mix and 27%, 20%, 25%, 20%, 23% for N2 mix, respectively. Meanwhile, the samples of N2 mix exhibits better compressive strength than that of N1 mix at all curing ages, which indicated that the amount of carbon content present in 1% of NCP char which slightly increased the interface of the cement matrix. It is also noteworthy that the high content of nano sized NCP char is also

favourable factor for the improved compressive strength. When NCP char was used as an additive to the cement, the super-hydrophobic nature and the stiffness difference between cement paste leads to weak matrix interface resulting in strength loss of cement paste cubes. Moreover, the hydrophobicity property of NCP char has poor bond strength resulting in cracks of cement matrix under external loads. In addition, the over-performance of the cement matrix is affected by reduced stiffness and elastic modulus of NCP char.

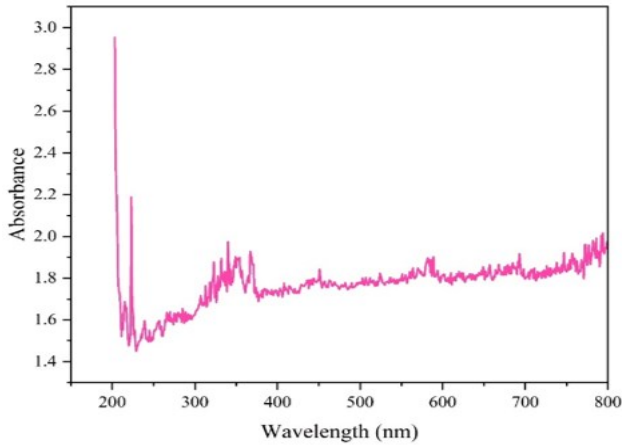


Figure 11. UV-Vis absorbance vs wavelength of NCP char

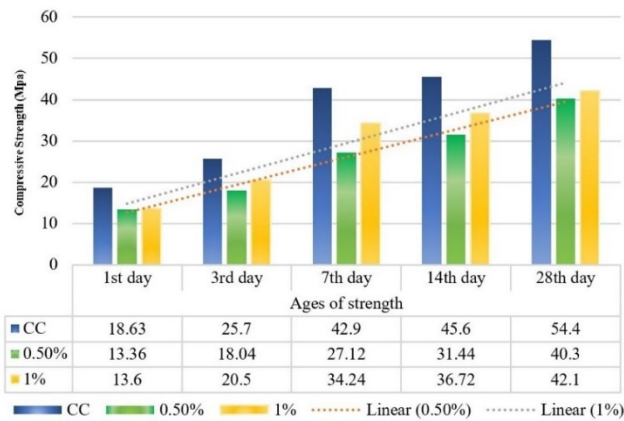


Figure 12. Compressive strength of NCP char incorporated cement paste matrix

6.2.2. Effects of compressive strength on dispersion process

The Figure 13a and 13b shows the effect of compressive strength on the cement paste matrix without and with dispersion technique. Primarily, the nano particles are complicated in dispersing into cement matrix and it is essential to adopt good dispersion technique depending on the nano-scale and material property (Kanagasundaram and Solaiyan 2023). The two major mechanism of dispersion process is to prevent the aggregation of NCP char and to distribute evenly among the cement matrix. It was found that the NCP char are hydrophobic in nature and not possible to disperse in the water. Consequently, by considering this property, NCP char were dispersed first mixed with ethanol and later dispersed with the combination of superplasticizer and water using magnetic stirrer as shown in the Figure 14. The cement matrix with dispersion technique exhibits increasing sophistication in the compressive strength comparing to cement matrix

without dispersion. Moreover, cement matrix without dispersion process confirms the unbalanced compressive strength at all ages for every mix which is due to aggregation of NCP char when it is added directly to the cement. Therefore, dispersion technique confirms the better interaction with cement matrix resulting in increased compressive strength at 28 days for all the mix proportions.

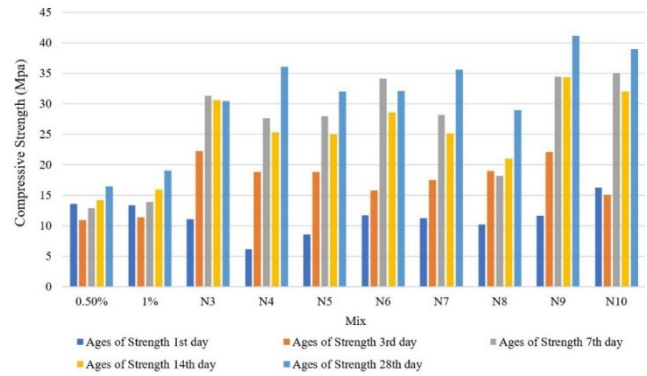


Figure 13. a) Compressive strength of cement paste matrix without dispersion

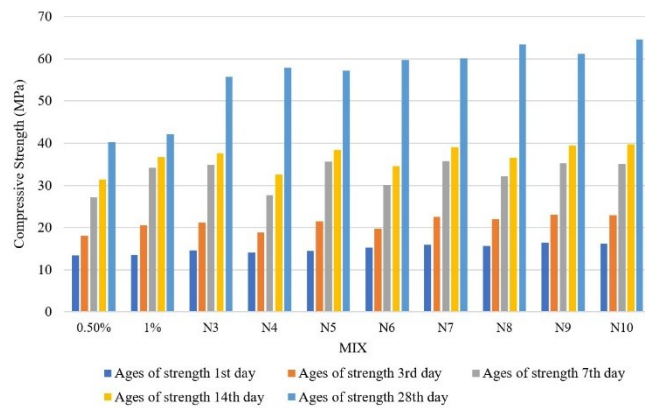


Figure 13. b) Compressive strength of cement paste matrix with dispersion

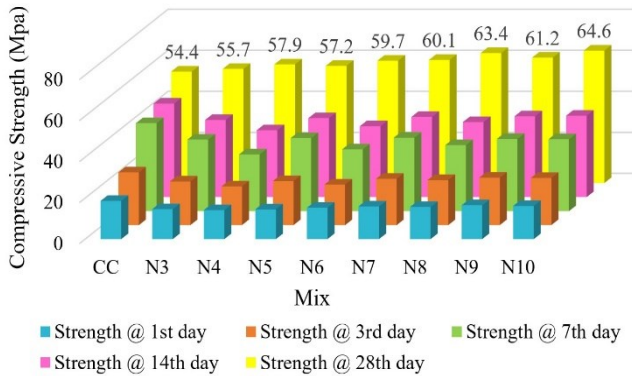


Figure 14. Dispersion of NCP char using magnetic stirrer

6.2.3. Effects of compressive strength on adding UPC with SF

The compressive strength of the cement paste matrix incorporated with different proportion of NCP char and SF after curing ages for 1 day, 3 days, 7 days, 14 days and 28 days was determined. From the Figure 15, it is observed that the compressive strength of cement paste cubes for all the mixes (N3 – N10) were improved when compared with

conventional mix (CC). Further, the compressive strength of N3, N4, N5, N6, N7, N8, N9, & N10 mix after curing for 28 days were increased by 2.4%, 6.4%, 5.1%, 9.7%, 10.5%, 16.5%, 12.5%, & 18.8%, respectively, compared to CC. Besides, the corresponding compressive strength at age of 1, 3, 7, & 14 days were lesser than the CC mix due to slow hydration process. Moreover, the compressive strength of the N4, N6, N8, & N10 mixes (1% of UPC + 2.5, 5, 7.5, & 10% of SF) were greater than the N3, N5, N7, & N9 mixes (0.5% of NCP char + 2.5, 5, 7.5, & 10% of SF), respectively. In addition, the increase in the SF dosage (i.e., high silica content) has effectively increased the strength of the matrix by dispersing the NCP char without agglomeration.



**Figure 15.** Compressive strength of cement paste matrix incorporated with UPC and SF

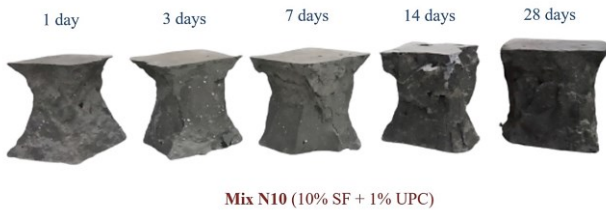


**Figure 16.** Ultimate failure pattern on the specimens after compressive loading

By comparing Figure 12 and 15, it is observed that the compressive strength of cement paste cubes mixed with UPC and SF exhibit better results than those of incorporating only NCP char. Therefore, the hybrid combination of micro-nano blends (SF and NCP char) demonstrates synergistic effect to improve the compressive strength of the specimen. This potent synergistic effect makes the sense of SF presence that played a significant role by preventing the agglomeration phenomena of nano particles and uniform distribution of NCP char. Meanwhile, SF also enhanced the adhesion properties and reduced the stratification of cement matrix. Once the silica fume is added to the cement matrix, firstly, it mechanically separates the NCP char from aggregation. Secondly, it reacts with  $\text{Ca}(\text{OH})_2$  present in the cement paste for the formation C-S-H. However, it takes time to reduces the concentration of calcium ions around the NCP char resulting in slow hydration process. In this regard, none of the specimens achieved the early strength and the failure pattern of mix N10 at different ages (1<sup>st</sup>, 3<sup>rd</sup>, 7<sup>th</sup>, 14<sup>th</sup>, & 28<sup>th</sup> day) is depicted in Figure 17. In addition, from the Figure 16 it is evident that the specimens at early age have minimum bonding and it progressively increased at 28

days. However, the compressive strength was significantly achieved for all the mixes at 28 days. Eventually from various mix proportions, N10 mix with 1% of NCP char and 10% of SF achieved the higher strength with sufficient bonding properties compared to CC and other mix proportions.

### 6.3. Durability properties

#### 6.3.1. Sorptivity

Sorptivity test is used to determine water absorption of cement composites with respect to time via capillary suction. Whereas, it is significantly affected by the physical characteristics and composition of cementitious materials in the matrix. In this study, the properties of NCP char and SF were the key factors that affected the capillary suction of the cement paste. In addition, incorporating only NCP char (N1-0.5% and N2-1%) exhibit poor contribution as the rate of absorption was very high compared to control mix (CC). On the other hand, synergistic effect of SF with NCP char (N3-N10) decreased the capillary absorption compared to CC mix and the highest reduction in the water absorption was observed in the Mix N10. The rate of absorption for all the mixes is shown in the Figure 17. Consequently, it is evidenced that the synergistic effect of SF and NCP char limited the absorption behaviour with less capillary pore diameter in the cement matrix. It is noteworthy that the nanomaterials (NCP) are effectively dispersed with SF to fill the pores in the microstructure and make the matrix denser.

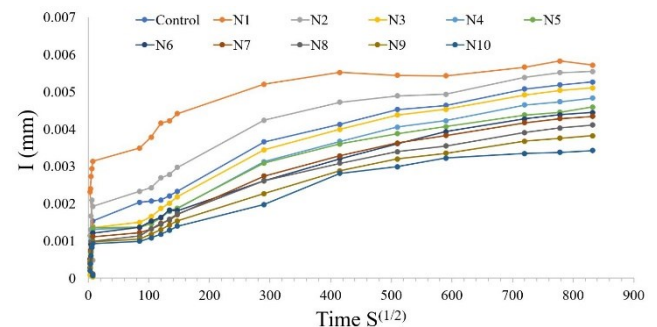


**Figure 17.** Sorptivity test on cement paste matrix

#### 6.3.2. RCPT

The RCPT was used to assess the resilience of a cement paste composite resistant to chloride ion penetration. From Figure 18, it is observed that the experimental results of sorptivity and RCPT are similar, where the mixes N1 and N2 exhibited high chloride ion permeability. The agglomeration of NCP particle resulting in porous structure is the reason for this high permeability. Further, the results demonstrated that the CC mix and the mixes incorporated up to 5% of SF and 1% of NCP char exhibited moderate chloride permeability. However, penetration of CC mix was higher than the other mixes. On the other hand, integrating 7.5% and 10% of SF with up to 1% of NCP char leading to low chloride ion permeability. The reduction in penetration is because of adsorption and retention of chloride ions, where the NCP char is well dispersed by SF in to the porous structure of cement paste matrix. Therefore, utilization of 1% of NCP char and 10% of SF induce to crucial reduction



in the charge passed, precisely below 2000 Coulombs because of the dense structure.

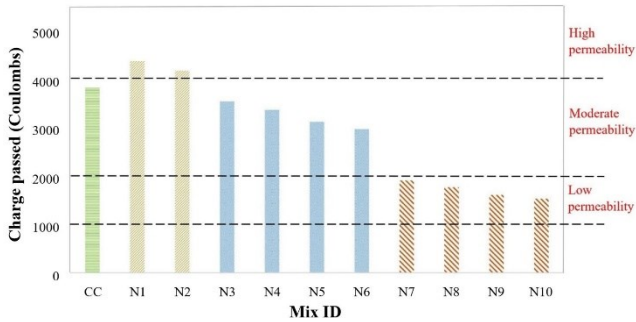


Figure 18. Rapid chloride permeability test values



Figure 19. Surface colour change of the specimen under acid exposure

6.3.3. Acid attack test

The nitric acid (2% concentration) having pH value of 3.2 was used for acid attack test. Initially, the specimens were visually examined and observed that the attack of HNO<sub>3</sub> has weakened the surface of cement composites and changed its colour to white as seen in Figure 19. Moreover, the surface crack was noticed due to leaching of calcium ions under HNO<sub>3</sub> solution. Further, it is anticipated to form shallow cracks at micro level on the surface of cement paste matrix because of tensile stress caused by acid attack. This differential stress was created on the decalcination process which induced shrinkage. Nevertheless, the core of cement paste matrix in all mixes were seemed to be unaltered by the nitric acid test. This exhibit the closed suboptimal packing of nano particles with significant amount SF content making the matrix susceptible to chemical attack. Subsequently, the mass loss on all specimens were measured and recorded as depicted in the Figure 20. It is perceived that the exposure of nitric acid had decreased the mass of specimen approximately by up to 3%. However, the mixes with NCP char and SF recorded less mass loss compared to CC, N1, & N2 mixes. Among the hybrid combination of nano/micro content, the

N9 & N10 mix have the least mass loss of 38.4% and 43.5%, respectively, compared to CC mix.

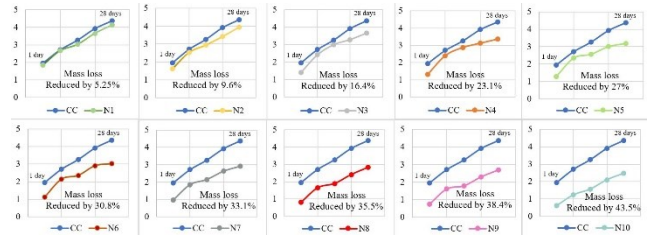


Figure 20. Acid test results for mass loss (%) vs curing age (days)

6.4. Microstructure properties

The core samples of conventional cement paste matrix (CC) and the cement composite with hybrid NCP char and SF (N10) were characterized by a formidable XRD technique to identify the various cement hydration products. Figure 21 represents the XRD pattern of CC and N10 mix after 28 days curing period. The XRD pattern indicates the various hydration phases in both the samples such as Portlandite/Ca (OH)<sub>2</sub>, Calcium-Silicate-Hydrate (C-S-H), Calcium Silicate (CS), Tricalcium Silicate (C<sub>3</sub>S), Ettringite/Calcium Sulphoaluminate, and Quartz (SiO<sub>2</sub>). Initially, it is observed that the N10 mix has no new phases compared to CC mix, indicating that the influence of NCP char and SF has not changed the structure of hydration products. By comparing the XRD patterns, it is apparent that the peak intensity of Portlandite (P) in N10 cement composite is lower than those in CC cement matrix, which exhibits the low crystalline degree of Ca (OH)<sub>2</sub> attributing to the good hydration process. Similarly, the ettringite peaks of N10 mix were also decreased compared to CC mix due to increase in C-S-H phase which inhibits the ettringite growth as evidenced at 2θ of 39.8°. Meanwhile, the peaks of SiO<sub>2</sub> content in N10 mix increases the C-S-H phase and it is responsible for providing good mechanical strength. Furthermore, the absence of unhydrated products such as C<sub>3</sub>S and CS in N10 cement composite indicate the increased hydration in the matrix.

The effect of NCP char with SF on the hydration of cement and hydrated morphology of cement composite was investigated by SEM. Figure 22a) and 22b) shows the micrograph of cement paste matrix after 28 days for CC mix and N10 mix, respectively. Both the mix produced good C-S-H formation but N10 cementitious paste produce high dense C-S-H hydration of type IV at low w/b = 0.29. The capillary pores observed in the CC mix were completed filled by NPC char with SF in the N10 mix and forms a secondary C-S-H (Vashistha *et al.* 2023) leading high compressive strength. Additionally, the Figure 22b) shows that the NCP char is well embedded into cement matrix and entangles in SF. Furthermore, the uniform distribution of SF in the microstructure implies a homogeneous dispersion of NCP char in the cementitious matrix. It is observed the numerous hydration products are appeared surrounding the NCP char indicating the strong interference between the particle of hydration product. Therefore, 10% of SF as a replacement contributes in the improvement of microstructure of cementitious matrix and dispersion of NCP char to provide high compressive strength.

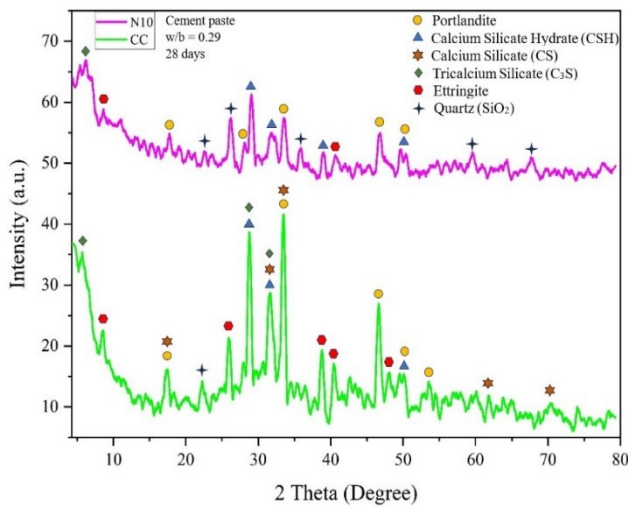


Figure 21. XRD patterns of plain cement paste and NPC/SF cement composite

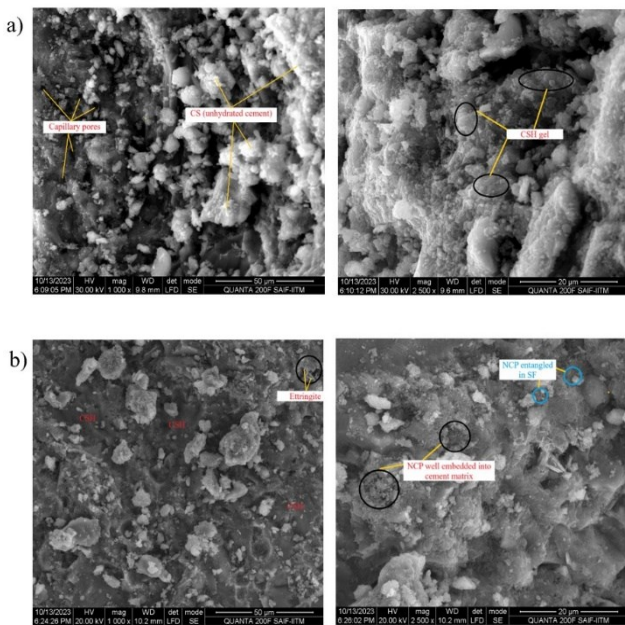


Figure 22. a) SEM micrograph of CC mix b) SEM micrograph of N10 mix

6.5. Finite element analysis

6.5.1. Modelling, meshing, and loading conditions

The 50mm x 50mm x 50mm cube is modelled for mixes CC and N10 using ANSYS Workbench software as shown in Figure 23a). Initially, the engineering data for both the cube models including the material properties were adopted from the experimental investigation and previous studies (Karthikeyan and Elavenil 2024). The meshing of the modelled cubes was executed by dividing into number of smaller elements as depicted in Figure 23b). Further, the models were subjected to compression loading to calculate the stress and deformation at integration point of these small elements. The required mesh density is selected based on trial solutions to avoid convergence issues. Once the model is created, it is ready to get discretized into fine mesh for further process in which the element type and shape is adopted as Solid 186 and quadrilateral, respectively, with default element size. The boundary condition is given as fixed support at bottom and the load

is applied at the top face. Loading is adopted using load-controlled scheme, in which load is the independent variable whereas displacement is the depended variable.

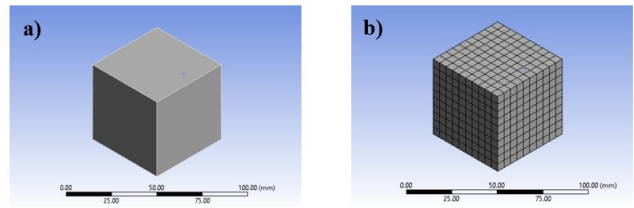


Figure 23. a) Finite element model of cement paste b) Meshed model of cement paste

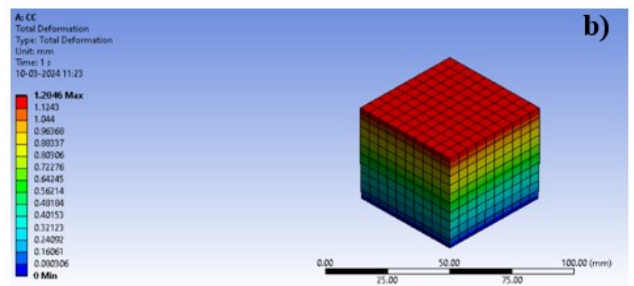
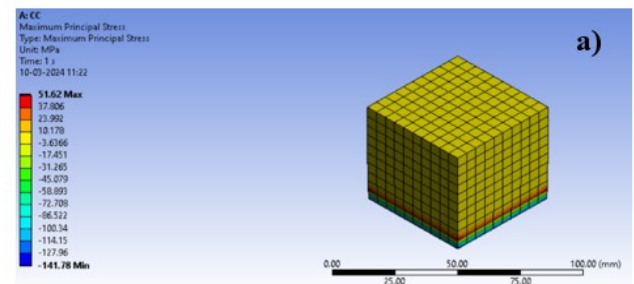


Figure 24. FEA results of CC mix a) maximum principal stress b) total deformation

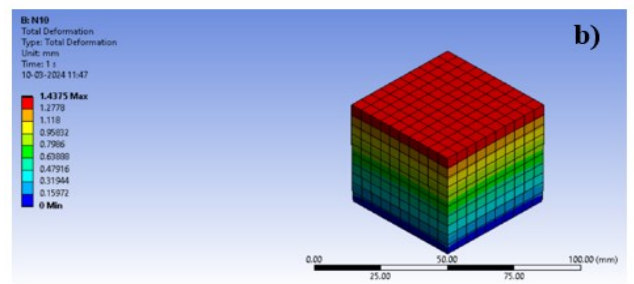
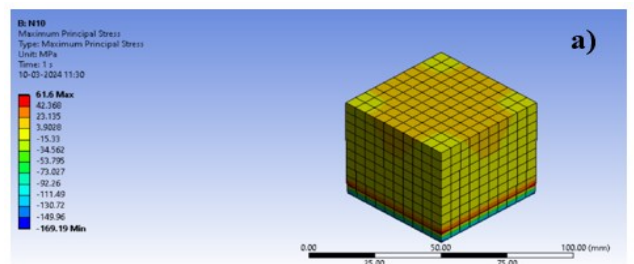


Figure 25. FEA results of N10 mix a) maximum principal stress b) total deformation

6.5.2. Analysis and validation

The FEA is carried out to study the analytical performance of CC and N10 cement paste matrix under compressive

loading. The major difference between these two models are the addition of material properties of NCP char and SF. The stress and deformation of the CC and N10 mix is depicted in Figure 24 and Figure 25, respectively. The analytical results clearly exhibit that the N10 mix have achieved high strength than the plain cement paste, CC. The NCP char containing nano size particles filled the pores of the plain cement paste making the suboptimal packing of particles resulting in higher density. Moreover, the mechanical, durability, and microstructure properties proved that the mixture of 1% of NCP char and 10% SF attained higher compressive strength with dense matrix and limited pores. With the experimental and analytical results, the density of N10 mix is seems to be higher compared to CC mix due to addition of nano/micro blends.

The experimental findings were compared with FEA models of the CC and N10 mix under compressive loading, as the Table 6 contrasts the stress and deformation of the FEA results with the experimental observations. However, the experimental failure pattern of N10 mix slightly differed to analytical failure model. Furthermore, the Figure 26

illustrates a comparison of the usual stress-deformation curves obtained from experimental and FEA results of CC and N10 mixes. The FEA resulted in 51.62 N/mm<sup>2</sup> and 61.6 N/mm<sup>2</sup> for CC and N10 mix, respectively, which is 2.78 N/mm<sup>2</sup> and 3 N/mm<sup>2</sup> lesser than experimental values. On the other hand, almost similar deformation values were identified for the both mixes. Therefore, the internal pattern of modelled cube satisfied the experimental mix procedure. From these results, it is showcased that the experimental to analytical results error percentage is less than 8% for both stress and deformation of CC and N10 mix. This indicates the FEA modelling and analysis is executed properly with well-defined material properties. From the aforementioned comparisons, it could be determined that the FEA and experimental findings generally reached good agreements. In light of this, parametric research on the CC and N10 mixes that goes beyond the scope of test specimens could be carried out using the FEA models.

**Table 6.** Validation results of CC and N10 cement paste cubes

| Specimen | Parameters  | Stress (MPa) | Deformation (mm) |
|----------|-------------|--------------|------------------|
| CC       | EXP         | 54.4         | 1.30             |
|          | FEA         | 51.62        | 1.21             |
|          | % Variation | 5.11         | 7.4              |
| N10      | EXP         | 64.6         | 1.53             |
|          | FEA         | 61.6         | 1.44             |
|          | % Variation | 4.87         | 6.3              |

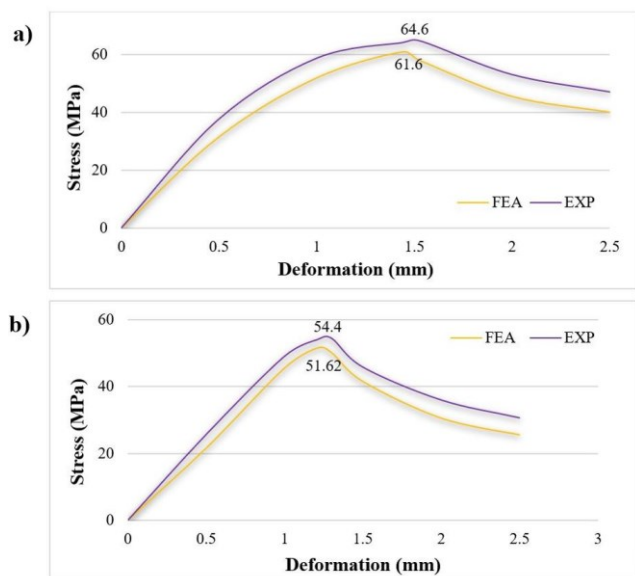


**Figure 26.** Experimental vs FEA results of stress-deformation curve a) CC b) N10

**7. Conclusion**

This research investigated the synergistic effect of NCP char and SF in various concentration on compressive, durability, and microstructural properties. In addition, the characterization of NCP char and SF were analysed by various microscopic and spectroscopic techniques to determine the standard of nano/micro blends. In this work, sustainable cement composites were developed using a

new sustainable nanomaterial (NCP char). Some salient conclusions investigated from this research are recapitulated as follows:

- The characterization techniques on NCP char confirmed the good surface area 29.5 m<sup>2</sup>/g and particle size of 56nm with high carbon content (>80%). Further, XRD confirms the pure and amorphous carbon present in the NCP char exhibiting an evolution of new sustainable carbon nano material. On the other hand, SF settled with high amorphous silica with no crystallinity having the potential to increase the strength of cement matrix.
- The complexity of dispersing nano particle into cement matrix is overwhelmed by the combination of hydrosol and first admixing dispersion method. This technique resisted the agglomeration of NCP char that maintained balanced compressive strength throughout the ages, while compared to the cementitious matrix without dispersion process.
- Individual effect of NCP char (0.5%) in cement matrix, decreased the compressive strength due to low bond strength and reduced stiffness resulting in weak matrix interface. However, it is noted that the increase in NCP char from 0.5% to 1% enhanced the compressive strength up to 5% owing to increase in carbon content.

- The synergistic effect of NCP char and SF improved the compressive strength of the matrix to 18.8% at 28 days of curing period. In addition, the SF played a potent role by separating the aggregation of nanoparticles and formations of C-S-H in large areas. The cement paste matrix with 1% of NCP char and 10% of SF attained better bonding and strength parameters compared to other mixes.
- Similarly, all the durability tests proved to be positive for the Mix N10 (1%NCP & 10%SF) when compared to other mixes resulting in less capillary pore diameter, low chloride ion permeability (1525 Coulombs), and minimum mass loss (2.47%).
- Microstructure properties observed from XRD and SEM exhibit homogeneous dispersion of NCP char, limited pores, and strong interaction between the materials and hydration products.
- FEA modelling validated with experimental findings indicated the error percentage of experimental to analytical results is less than 8% for both stress (MPa) and deformation (mm).

#### Recommendation to future direction

- Sustainable Nano-carbon Pyrolytic char as a nano carbon functional filler has wide opened the multiple gaps do develop sustainable nano composites with multifunctional properties.
- The effect on higher concentration and size reduction of sustainable NCP char can be investigated for engineering properties.
- The NCP char with high carbon content has the ability to improve electrical resistivity, conductivity, and may be for self-sensing applications.

#### Acknowledgement

Authors would like to thank the Dean-School of Civil Engineering, Vellore Institute of Technology, Chennai, India for providing support and lab facilities to carry out this research. We thank the "DST and SAIF/IIT/M", "School of Advanced Sciences, VIT-Chennai", for providing the analytical services.

#### References

- Al-Subari L., Ekinici A. and Aydin E. (2021). The utilization of waste rubber tire powder to improve the mechanical properties of cement-clay composites, *Construction and Building Materials*, **300**, 124306.
- Chen B., Guo L. and Sun W. (2014). Fatigue performance and multiscale mechanisms of concrete toughened by polymers and waste rubber, *Advances in Materials Science and Engineering*, **2014**, 684207.
- Dong W., Li W., Guo Y., He X. and Sheng D. (2020). Effects of silica fume on physicochemical properties and piezoresistivity of intelligent carbon black-cementitious composites, *Construction and Building Materials*, **259**, 120399.
- Friedlingstein., Andrew. and Peters. (2023). Statistic Id1091672 Global Carbon Dioxide Emissions From Cement Manufacturing 1990–2021. <https://www.statista.com/statistics/1091672/carbon>.
- Gao P., Wang Y., Wang Y., Zhou H. and Xue G. (2023). Influence of waste tire rubber powder, polypropylene fiber and their binary blends on mitigating alkali-silica reaction, *Journal of Building Engineering*, **67**, 105951.
- Gil-Martín L. M., Rodríguez-Suesca A. E., Fernández-Ruiz M. A. and Hernández-Montes E. (2019). Cyclic behavior of RC beam-column joints with epoxy resin and ground tire rubber as partial cement replacement, *Constructions and Building Materials*, **211**, 659–674.
- Hamdi A., Abdelaziz G. and Farhan K. Z. (2021). Scope of reusing waste shredded tires in concrete and cementitious composite materials: A review, *Journal of Building Engineering*, **35**, 102014.
- He J., Guo T., Li Z., Gao Y. and Zhang J. (2024). Hydration mechanism of red mud-fly ash based geopolymer. *Materials Chemistry and Physics*.
- Huang C., Hong J., Lin J., Deng C. and Li L. (2014). Utilization of waste rubber powder in semi-flexible pavement, *Key Engineering Materials*, **599**, 361–367.
- Jegatheeswaran D., Sridhar J., Saranya S., Gokulan R. and Gasim H. (2023). Utilization of nanomaterials and ceramic waste for sustainable environmental protection, *Global Nest Journal*, **25**, 51–59.
- Kanagasundaram K. and Solaiyan E. (2023). Smart cement-sensor composite : The evolution of nanomaterial in developing sensor for structural integrity, *Structural Concrete*, **24**, 6297–6337.
- Karthikeyan G., Leema M. A., Muruganantham R. and Harshani R. (2024). Influence of utilizing prosopis juliflora ash as cement on mechanical properties of cement mortar and concrete, *Global Nest Journal*, **26**, 05402.
- Karthikeyan N. K. and Elavenil S. (2024). Characterization of nano-structure pyrolytic char for smart and sustainable nanomaterials, *Advances in Nano Research*, **16**, 53–69.
- Khater H. M. (2013). Effect of silica fume on the characterization of the geopolymer materials. *International Journal of Advanced Structural Engineering*, **5**, 1–10.
- Kim G. M., Kim Y. K., Kim Y. J., Seo J. H., Yang B. J. and Lee H. K. (2019). Enhancement of the modulus of compression of calcium silicate hydrates via covalent synthesis of CNT and silica fume, *Construction and Building Materials*, **198**, 218–225.
- Kirthiga R. and Elavenil S. (2022). A review on using inorganic binders in fiber reinforced polymer at different conditions to strengthen reinforced concrete beams, *Construction and Building Materials*, **352**, 129054.
- Kouimtzi M. and Kostopoulou S. (2023). Interaction of pyrolysis conditions and soil texture on biochar, *Global Nest Journal*, **25**, 9–16.
- Liu W., Du H., Yi P., Li Y., Luo Y., Chen Q. and Xing F. (2023). The early hydration and rheological characteristics of cement paste containing co-combustion fly ash, *Journal of Building Engineering*, **78**, 107736.
- Lokesh R., Pandian M. S., Karthikeyan, N. K. and Hema N. (2023). Performance of different post tensioning slab system and its environmental constraints, *AIP Conference Proceedings*, **2764**, 50008.

- Luo D. and Wei J. (2023). Hydration and phase evolution of blended cement composites containing lithium and saturated metakaolin, *Cement and Concrete Composites*, **144**, 105268.
- Luo T., Hua C., Liu F., Sun Q., Yi Y. and Pan X. (2022). Effect of adding solid waste silica fume as a cement paste replacement on the properties of fresh and hardened concrete, *Case Studies in Construction Materials*, **16**, e01048.
- Ma X., He T., Xu Y., Yang R. and Sun Y. (2022). Hydration reaction and compressive strength of small amount of silica fume on cement-fly ash matrix, *Case Studies in Construction Materials*, **16**, e00989.
- Meyer C. (2009). The greening of the concrete industry, *Cement and Concrete Composites*, **31**, 601–605.
- Murali G., Katman H.Y.B., Wong L.S., Ibrahim M.R., Ramkumar V.R. and Abid S.R. (2023). Effect of recycled lime sludge, calcined clay and silica fume blended binder-based fibrous concrete with superior impact strength and fracture toughness, *Construction and Building Materials*, **409**, 133880.
- Nalon G.H., Santos R.F., Lima G.E.S. de Andrade I.K.R., Pedroti L.G., Ribeiro J.C.L. and de Carvalho J.M.F. (2022). Recycling waste materials to produce self-sensing concretes for smart and sustainable structures: A review, *Construction and Building Materials*, **325**, 126658.
- Arasu A., Natarajan M., Balasundaram N. and Parthasaarathi R. (2023). Utilizing recycled nanomaterials as a partial replacement for cement to create high-performance concrete, *Global Nest Journal*, **25**, 89–92.
- Nogueira M., Matos I., Bernardo M., Pinto F., Lapa N., Surra E. and Fonseca I. (2019). Char from Spent Tire Rubber: A Potential Adsorbent of Remazol Yellow Dye, *Journal of Carbon Research*, **5**, 76.
- Reyna S.L.R., Domínguez, O., Aguilera J.H.D. and García C. (2021). Synergistic effects of rubber-tire-powder and fluorogypsum in cement-based composite, *Case Studies in Construction Materials*, **14**, e00471.
- Ren F., Mo J., Wang Q. and Ho J. C. M. (2022). Crumb rubber as partial replacement for fine aggregate in concrete: An overview, *Construction and Building Materials*, **343**, 128049.
- Shanmuga Priya S. and Padmanaban I. (2024). Effect of coconut shell ash as an additive on the properties of green concrete, *Global Nest Journal*, **26**, 05413.
- Shilpa, Kumar R. and Sharma A. (2018). Morphologically tailored activated carbon derived from waste tires as high-performance anode for Li-ion battery, *Journal of Applied Electrochemistry*, **48**, 1–13.
- Valentini F. and Pegoretti A. (2022). End-of-life options of tyres : A review, *Advanced Industrial and Engineering Polymer Research*, **5**, 203–213.
- Vashistha P., Oinam Y. and Pyo S. (2023). Valorization of waste concrete powder (WCP) through silica fume incorporation to enhance the reactivity and hydration characteristics, *Development in Built Environment*, **16**, 100272.
- Wang M., Zhang L., Li A., Irfan M., Du Y. and Di W. (2019). Comparative pyrolysis behaviors of tire tread and side wall from waste tire and characterization of the resulting chars. *Journal of Environmental Management*, **232**, 364–371.
- Wang Y. and Wang X. (2023). Multi-characterizations of the hydration, microstructure, and mechanical properties of a biochar-limestone-calcined clay-cement (LC<sup>3</sup>) mixture, *Journal of Materials Research and Technology*, **24**, 3691–3703.
- WBCSD (2019). Global ELT Management: A global state of knowledge on regulation, management systems, impacts of recovery and technologies. Available at: [https://docs.wbcsd.org/2019/12/Global\\_ELT\\_Management-A\\_global\\_state\\_of\\_knowledge\\_on\\_regulation\\_management\\_systems\\_impacts\\_of\\_recovery\\_and\\_technologies.pdf](https://docs.wbcsd.org/2019/12/Global_ELT_Management-A_global_state_of_knowledge_on_regulation_management_systems_impacts_of_recovery_and_technologies.pdf).
- Xia Y., Liu M., Zhao Y., Chi X., Guo J., Du D. and Du J. (2023). Hydration of ternary blended cements with sewage sludge ash and limestone: Hydration mechanism and phase assemblage, *Construction and Building Materials*, **375**, 130868.
- Zafar I., Rashid K., Tariq S., Ali A. and Ju M. (2022). Integrating technical environmental economical perspectives for optimizing rubber content in concrete by multi-criteria analysis, *Construction and Building Materials*, **319**, 125820.
- Zhang R., Wang H., Ji J., Suo Z. and Ou Z. (2022). Influences of different modification methods on surface activation of waste tire rubber powder applied in cement-based materials, *Construction and Building Materials*, **314**, 125191.
- Zhang Y., Chang J., Zhao Q., Lam W. L., Shen P., Sun Y., Zhao D. and Poon C.S. (2022b). Effect of dosage of silica fume on the macro-performance and micro/nanostructure of seawater Portland cement pastes prepared with an ultra-low water-to-binder ratio, *Cement and Concrete Composites*, **133**, 104700.
- Zhang Y., Chen Y. and Çopuroğlu O. (2023). Effect of P<sub>2</sub>O<sub>5</sub> incorporated in slag on the hydration characteristics of cement-slag system, *Constructions and Building Materials*, **377**, 131140.
- Zhao J., Wang D., Wang X., Liao S. and Lin H. (2015). Ultrafine grinding of fly ash with grinding aids: Impact on particle characteristics of ultrafine fly ash and properties of blended cement containing ultrafine fly ash, *Constructions and Building Materials*, **78**, 250–259.
- Zhu Y., Zhang Z., Yang Y. and Yao Y. (2014). Measurement and correlation of ductility and compressive strength for engineered cementitious composites (ECC) produced by binary and ternary systems of binder materials: Fly ash, slag, silica fume and cement, *Constructions and Building Materials*, **68**, 192–198.